Filtering methods for different characteristic stripe noise in SAR image

KOU Guangjie[1,2,3], WANG Zhensong[1], YAO Ping[1]

1. *Institute of Computing Technology, Chinese Academy of Sciences, Beijing* 100190, *China*;
2. *Graduate School, Chinese Academy of Sciences, Beijing* 100049, *China*;
3. *School of Information Science and Engineering, Ludong University, Shandong Yantai* 264025, *China*

Abstract: We analize the reason of periodic bright and shadow stripe noise generated in burst mode SAR, when the full aperture imaging algorithm is used. A simple but efficient one-dimensional frequency domain filtering method is proposed along with the flow chart of improved Range Doppler imaging algorithm including this operation. We discuss the nonperiodic abnormal stripe noise due to the spaceborne SAR system itself, and present an area filtering method in two-dimensional frequency domain. The validities of the algorithms in the paper are proved by processing actual spaceborne SAR data.

Key words: Range Doppler algorithm, stripe noise, frequency domain filtering, burst mode

CLC number: TP751/TN958 **Document code:** A

Citation format: Kou G J, Wang Z S and Yao P. 2011. Filtering methods for different characteristic stripe noise in SAR image. *Journal of Remote Sensing*, **15**(1): 1–12

1 INTRODUCTION

Spaceborne synthetic aperture radar (SAR) is a kind of active microwave sensor which can work at any time in any weather, and be widely used nowadays in all fields of earth observation. Some periodic or nonperiodic stripe noises, which greatly affect the image quality and subsequent application, may appear in SAR images because of the signal processing algorithms or SAR system itself. Thus, to look for a simple and effective SAR image denoising algorithms becomes more significant. However, the properties of SAR image are different from optical image according to the coherent imaging principle. For example, there exists the speckle noise. Hence, the common denoising algorithms for optical image can not be utilized in SAR image directly. Some studies about the stripe noise in SAR image have been done by Lou, *et al.* (1999), on the basic of which two more simple and efficient denoising algorithms are proposed in the paper through the classification of the noise.

When the full aperture algorithm is used to process burst mode spaceborne SAR data, the first kind stripe noise appears for the additional modulation noise introduced by zeros patching between effective bursts (Cumming, *et al.*, 2005; Hlzner, *et al.*, 2002). Periodic bright and shadow vertical stripes will appear on the final imaging results. Taking the filtering methods for periodic noise in optical image (Aizenberg, *et al.*, 2008; Chen, *et al.*, 2003; Ghada, *et al.*, 2005; Preesan, *et al.*, 2009; Tsai, *et al.*, 2008; Liu, *et al.*, 2006) as the references, the paper proposes a simple but efficient one-dimensional median filter in frequency domain. The frequencies corresponding to the stripe noises are determined by the average value of multiple azimuth lines in frequency domain, so the coherent interference in SAR image can be reduced maximally. The computational efficiency is improved comprehensively greater than conventional two-dimensional frequency domain filters. Furthermore, it can be easily combined with RD algorithm, and the better computational efficiency can be obtained. The flowchart of this improved RD algorithm is presented in the paper. The validity of this algorithm is proved by processing ENVISAT SAR data.

Nonperiodic irregular stripe noise may be generated because of SAR system itself or external interference and it is the second stripe noise discussed in the paper. For this more complex noise, after analyzing the relation between grayscale image in time domain and amplitude image in frequency domain, the paper proposes an interactive area filtering algorithm in two-dimensional frequency domain. The validity of this algorithm is also proved by processing actual spaceborne SAR data.

2 THEORETICAL BASIS OF STRIPE NOISE FILTERING ALGORITHMS

Two-dimensional Fourier transform is an orthogonal transform, and it can decompose the image to a series of sine

Received: 2010-01-21; **Accepted**: 2010-06-02

Foundation: The 11th Five-Year Plan national defense advanced research project.

First author biography: KOU Guangjie (1977—), male, Lecturer, He is currently pursuing the Ph.D degree at the Institute of Computing Technology, Chinese Academy of Sciences. His research interests include SAR signal processing and image processing. E-mail: kouguangjie@ict.ac.cn

and cosine signals. Thus, it is widely used in image analysis, filtering, compression and reconstruction etc.. The energy distribution is gathered to low-frequency components by the transform, while the detailed information of the image edges and lines is reflected on high frequency components. If the orientations of the objects in time domain image have regularities, the orthogonal direction properties will appear on the high amplitude spectrum too. This conclusion can be proved as following. Assuming the distributing mode of gray image $f(x,y)$ in time domain is extended along y axis, and it can be expressed as

$$f(x,y)=\begin{cases}A & 0\leqslant x\leqslant X, 0\leqslant y\leqslant Y\\ 0 & \text{others}\end{cases} \tag{1}$$

where A is amplitude of the gray level image, X、Y are pixel numbers along horizontal and vertical ordinates, $X<<Y$. The Fourier transform of $f(x,y)$ is

$$F(u,v)=AXY\times\left|\frac{\sin(\pi uX)\times\exp(-j\pi uX)}{\pi uX}\right|\times\left|\frac{\sin(\pi vY)\times\exp(-j\pi vY)}{\pi vY}\right| \tag{2}$$

And the corresponding amplitude spectrum is

$$|F(u,v)|=AXY\times\left|\frac{\sin(\pi uX)}{\pi uX}\right|\times\left|\frac{\sin(\pi vY)}{\pi vY}\right| \tag{3}$$

Since $1/X>>1/Y$, the spectral amplitude mode extends along u axis. That is to say the extending direction of the spectral amplitude mode is orthogonal with the extending direction of the gray image in time domain. The conclusion is still valid to the general image pattern and it can be proved by the scale transform property Eq.(4) and the rotation property Eq.(5) of the two-dimensional Fourier transform.

$$\mathrm{FFT}\{f(ax,by)\}=\frac{F(u/a,v/b)}{|ab|} \tag{4}$$

$$\mathrm{FFT}\{f(x\cos\theta-y\sin\theta,x\sin\theta+y\cos\theta)\}=F(u\cos\theta-v\sin\theta,u\sin\theta+v\cos\theta) \tag{5}$$

where $FFT\{f\}$ denotes the two-dimensional Fourier transform of function $f(x,y)$, which a,b and θ are constants. Thus, the amplitude shape in frequency domain can be determined by the shape of stripe noises in time domain, and then the target of noise reduction can be achieved by corresponding process. This is the foundation of frequency noise filter design in the paper.

3 PERIODIC STRIPE NOISE FILTERING IN SAR IMAGE

3.1 Analysis of periodic stripe noise

To apply full aperture imaging algorithms in burst mode SAR, zeros should be patched between effective bursts firstly. Then, the time relationship corresponding to stripmap SAR is obtained, and the common stripmap SAR imaging algorithms can be used. The zero patching is equivalent to multiply a fixed time rectangle signal (the value is zero) to the conventional stripmap SAR data. Thereby, a periodic noise along azimuth direction is introduced. This noise has significant influence on the range and azimuth decoupled imaging algorithms (such as RD), and some bright and shadow stripes will appear on the final SAR image (Curlander, *et al.*, 1991; Ding, *et al.*, 2002; Hlzner, *et al.*, 2002). The effect is similar to the imaging results of uneven weighted antenna directional pattern. Since the stripe noise extends along range direction and appears periodically in azimuth direction, the spectral amplitude mode must be extended in azimuth direction based on the conclusion of section 2.

If the cycle and width of the stripe noise is fixed, a couple of symmetric impulses along azimuth direction in two-dimensional frequency domain will be generated, where the frequencies of the impulses are determined by the cycle of noise. The noise can be removed in two-dimensional frequency domain by conventional optical image processing methods such as notch filter (Gonzalez, *et al.*,2001), Gauss weighted notch filter (Aizenberg, *et al.*,2008) or median filter (Ghada, *et al.*,2005; Zhang, *et al.*,2002; Lin, *et al.*, 2007; Chang, *et al.*,2008). Since the stripe noise has regular shape and fixed cycle, the noise reduction process does not need to completely change the image into two-dimensional frequency domain and only one-dimensional Fourier transform along perpendicular direction to the stripe noise can meet the requirement. Thus, a one-dimensional frequency domain filter for periodic stripe noise in SAR image is proposed.

3.2 Periodic stripe noise filtering method

Since the spectral powers of the stripe noise and the nature scene are mixed together and the influence of coherent noise exists simultaneously, the frequencies of stripe noise cannot be determined by a single azimuth line. If we accumulate all the azimuth lines, the spectral powers corresponding to the nature scene are restrained by each other and it can not become very large. But the peaks of spectral powers corresponding to stripe noise will be generated: Except the zero frequency, other peaks may be corresponding to the frequencies of stripe noise. Assume there are M points in azimuth direction and N points in range direction. The vector $\boldsymbol{F}_x$ denotes the Fourier transform result of the xth azimuth line, $\boldsymbol{P}_x$ is the Fourier amplitude spectrum of $\boldsymbol{F}_x$, $x=1,\ldots,N$. Steps of one-dimensional frequency domain filter are listed as follows.

Step 1 Mean value of azimuth lines Fourier spectrum can be obtained by Eq.(6).

$$\boldsymbol{MeanSpect}=\frac{1}{N}\times\sum_{x=1}^{N}\boldsymbol{P}_x \tag{6}$$

where

$$\boldsymbol{P}_x=|\boldsymbol{F}_x| \tag{7}$$

$$\boldsymbol{F}_x(v)=\frac{1}{M}\times\sum_{y=0}^{M-1}f(x,y)\times\exp(-j2\pi vy/M) \tag{8}$$

Step 2 Seek for the peaks of *MeanSpect* except the zero frequency.

Symmetrical spectral power peaks, which are frequencies of the stripe noise, are found and is denoted as f_{noise} uniformly. To determine the noise frequencies by the peak search is independent of SAR parameters and unaffected by image resampling. Thus the stripe noise filtering becomes a universal operation.

Step 3 According to the noise frequency f_{noise}, each azimuth line is processed by the one-dimensional median filter Eq.(9).

$$\boldsymbol{F}(f_{\text{noise}}) = \text{median}\{\boldsymbol{F}(v)/\delta\} \tag{9}$$

The function median substitutes the Fourier spectrum amplitude at f_{noise} by the median value in a one-dimensional window but keeps the phase values unchanged. δ is a destriping factor. Since actual scenes information exist at f_{noise} too, some image information will be lost if the corresponding amplitude value is set to zero directly. A weighted one-dimensional median filter is adopted in the method.

Step 4 Utilize the inverse Fourier transform on the frequency domain image obtained in Step 3, and the recovered image is obtained.

3.3 The improved RD algorithm which includes the stripe noise filter

As the preceding stripe noise filter can be realized in one-dimensional frequency domain, the analysis of RD flowchart shows that if the filter is added into RD algorithm prior to the last IFFT step, the same performance can be obtained while the computation efficiency is improved further. The flowcharts of RD with and without the filter are displayed in Fig. 1.

The parameters of SAR system (such as burst duration time, PRF, time correspondent with zeros patching etc.) can be obtained during the imaging process. Under this condition, the frequency of the stripe noise can be achieved by simple calculation. Thus the accumulation of all the azimuth lines is not necessary.

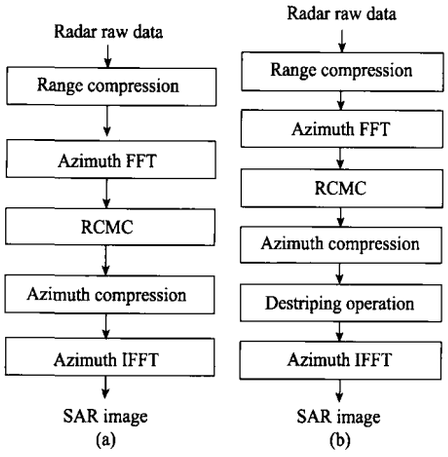

Fig. 1 The flowcharts of RD algorithm before and after improving
(a) Conventional RD algorithm; (b) Improved RD algorithm

4 NONPERIODIC STRIPE NOISE FILTERING

4.1 Analysis of nonperiodic stripe noise

Another stripe noise generated by SAR system itself or external interference may appear on SAR image. It is typically nonperiodic and associated with targets. Furthermore the length and width of every stripe are different (Fig.4 (a), (d)). As the stripe noises have various length and are not through the whole picture, the frequencies of the noises can not be determined by the method in section 3 and the conventional two-dimensional frequency domain filters are invalid (Gonzalez, *et al.*, 2001; Aizenberg, *et al.*, 2008; Ghada, *et al.*, 2005) too. A two-dimensional frequency domain area filtering method is proposed based on the following idea. Firstly, the area corresponding to stripe noise in the spectrum image is determined by the conclusion in section 2 that the distributions of amplitude in spectrum image and grayscale image are perpendicular. Secondly, the stripe noise is removed by the corresponding processing on this area.

4.2 Determination of the area corresponding to the noise in spectrum image

Although this kind of stripe noise seems in a clutter, there still exist some common features: extending along vertical direction, nonperiodic, variational stripe width. Conclusion of section 2 shows that the energy distribution of this kind noise should extend along horizontal direction and may appear on all the frequency because of the nonperiodic attribution. Hence, a bright line may be found in the spectrum image. As the widths of every stripe are different, the width of the bright line in spectrum image is not one pixel. The spectrum image (such as Fig.4(g)) can be obtained by two-dimensional Fourier transform, and a bright line with the width of about five pixels appear in the middle of the image. So, the preceding analysis is confirmed too. The area corresponding to the noise in the spectrum image is determined now, and the noise can be removed by suitable adjusting to these data.

4.3 Specific steps of the filtering method for irregular stripe noise

Step 1 Utilize two-dimensional Fourier transform on the input-image, and display the spectrum image. To see detailed information clearly, the logarithm transform may be used firstly.

Step 2 Determine the area corresponding to vertical stripes in the spectrum image obtained by step 1.

Step 3 The values of spectrum amplitude inside the area determined in Step 2 are substituted by the mean values of the two sides adjacent to the bright line. The phase values should keep unchanged.

Step 4 Utilize two-dimensional inverse Fourier transform on the image obtained from Step 3 and then the recovered

image is obtained.

5 EXPERIMENT

5.1 Periodic stripe noise filtering in SAR image

ENVISAT is one of the Earth observation satellites of European Space Agency. It is launched on Mar. 1st 2002, on which there are many sensors to observe the land, sea and air separately. As the main sensor among them, the synthetic aperture radar ASAR works at C-band and has the characteristics of multi-polarization, multiple look angles, and wide swath imaging etc.. Apply full aperture RD algorithm on the burst mode raw data, the level 1 image and corresponding filtering results are displayed in Fig. 2.

Two SAR images with stripe noise are displayed in Fig. 2(a) and Fig.2(d), and the image quality is degraded greatly because of the obvious periodic energy variation along azimuth. The filtering results with method proposed in section 3 are presented in Fig. 2(b) and Fig.2 (e), where the window size of the one dimensional median filter is 7 and σ is 5. The removed stripe noises are displayed in Fig. 2(c) and Fig.2 (f). The vectors of the mean azimuth spectrum *MeanSpect*, corresponding to scene 1, with and without filtering the stripe noise are displayed in Fig. 3, where the abscissa is normalized frequency and only half cycle spectrum line is given. The peak value corresponding to the noise is removed efficiently.

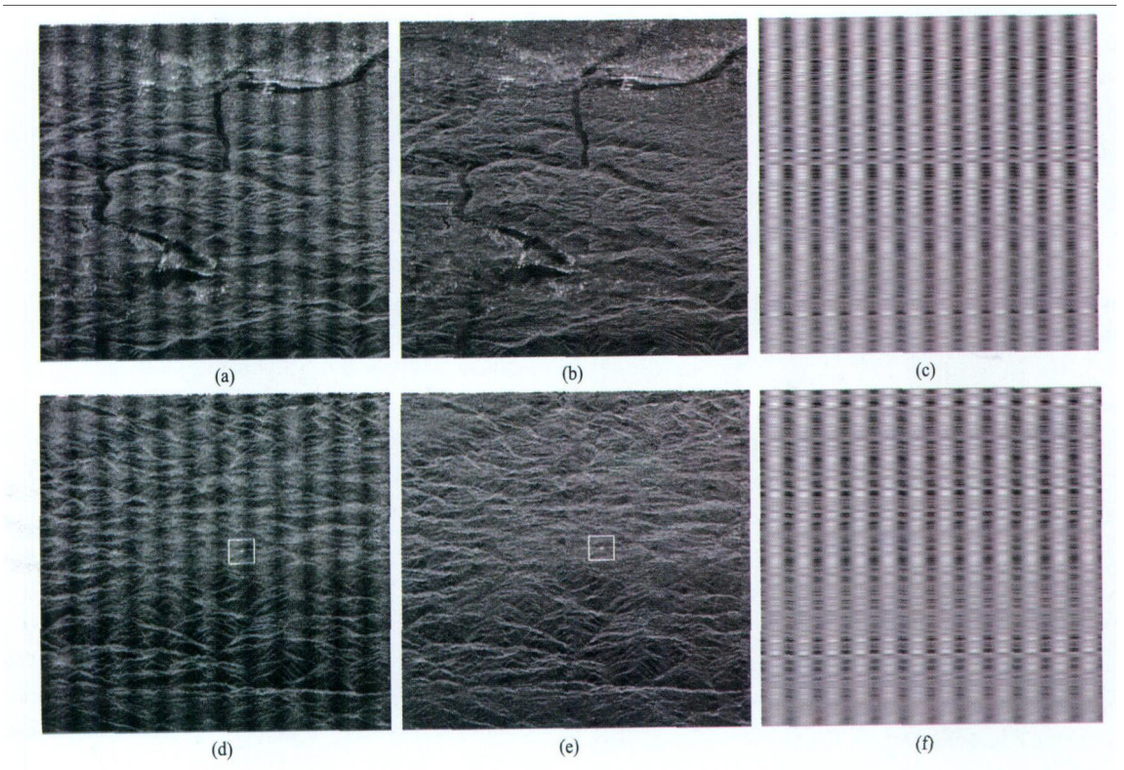

Fig. 2 Filtering results of the periodic stripe noise; image size is 512×512 pixels
(a) Before filtering the stripe noise of Scene 1; (b) After filtering the stripe noise of Scene 1; (c) The filtered stripe noise from Scene 1; (d) Before filtering the stripe noise of Scene 2; (e) After filtering the stripe noise of Scene 2; (f) The filtered stripe noise from Scene 2

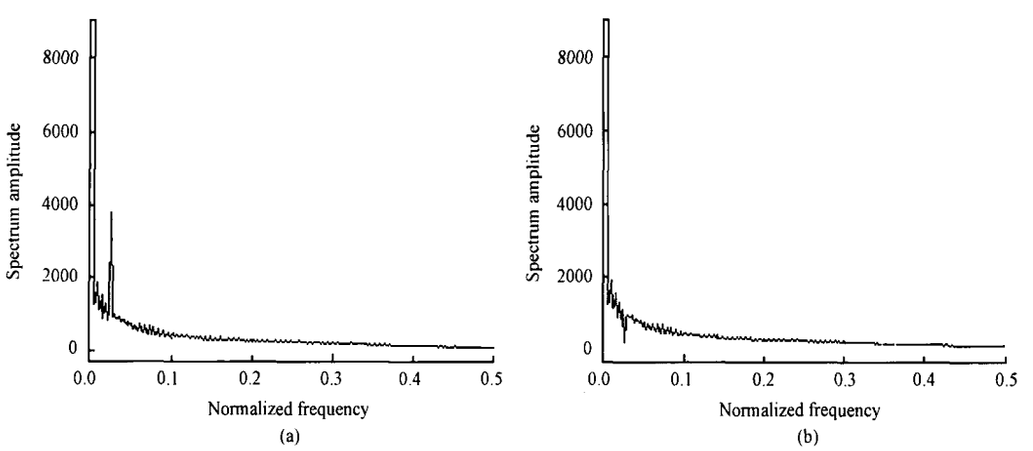

Fig. 3 The change of azimuth spectrum mean value in Scene 1 before and after filtering the noise
(a) Azimuth spectrum with stripe noise; (b) Azimuth spectrum after filtering the stripe noise

5.2 Irregular stripe noise filtering in SAR image

Fig. 4 displays the level 1A images of Dubai district processed by RD algorithm from another stripmap spaceborne SAR. Fig.4(a) and Fig.4(d) are images with stripe noise. Although the gaps among these stripes seem small, the result is poor if the low pass filter is applied on the noise image directly. As an example, Fig.4(i) displays the filtering results of Fig.4(a) with Gauss low pass filter. The stripe noise still exists even though the image becomes blurred. Thus this kind of filters is invalid already. Appling one-dimensional frequency domain filter discussed in section 3 on the image with noise, there is no obvious peak after the accumulation and the frequency corresponding to the noise can not be determined, which verifies the analysis in section 4.1 further. Filtering results with method proposed in section 4.3 are displayed in Fig.4(b) and Fig.4(e), and the removed noises are presented in Fig.4(c) and Fig.4(f). Apparently, the stripe noises are filtered effectively. Fig.4(g) and Fig.4(h) display the spectrum images before and after filtering.

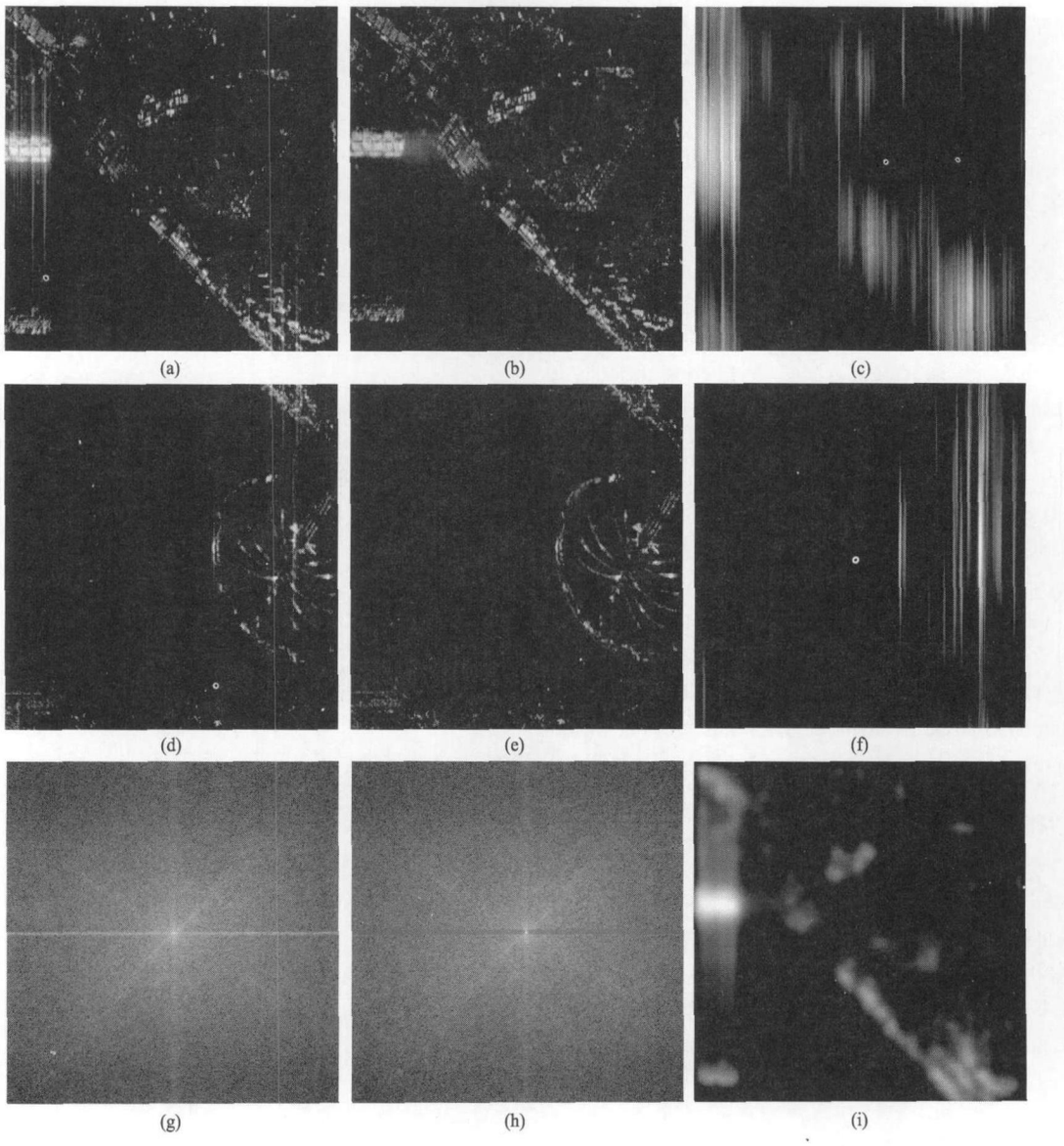

Fig. 4 Filtering results of nonperiodic stripe noise (image size is 256×256 pixels)

(a) Before filtering the stripe noise of Scene 3; (b) After filtering the stripe noise of Scene 3; (c) The filtered stripe noise from Scene 3; (d) Before filtering the stripe noise of Scene 4; (e) After filtering the stripe noise of Scene 4; (f) The filtered stripe noise from Scene 4; (g) The spectrum amplitude before filtering the noise of Scene 3; (h) The spectrum amplitude after filtering the noise of Scene 3; (i) Filtering result with low pass filter of Scene 3

5.3 Evaluation of the noise reduction

In addition to the visual effects of the images, the noise reduction ratio (*NR*) (Preesan, *et al.*, 2009; Chen, *et al.*,2003) and the change of image resolution are employed as quality indexes to evaluate the noise reduction methods. *NR* is calculated from Eq.(10).

$$NR=N_0/N_k \tag{10}$$

where N_0 stands for the power of the frequency components produced by stripe noise in the original image, and N_k stands for the corresponding power in the destriped image. *NR* reflects the degree of noise reduction. The values of *NR* corresponding to

the preceding four images are listed in Table 1.

Table 1 Noise reduction ratio *NR*

Image	*NR*	Image	*NR*
Scene 1	18.69	Scene 3	26.36
Scene 2	19.17	Scene 4	19.26

The change of image resolution is measured by the pixel number variation of a strong reflectance target before and after noise reduction. For example, a strong reflectance target in scene 2 is included in a 20×20 pixels window and the target has eight pixels before and after noise reduction. That is to say, the resolution is not degraded significantly with the stripe noise filtering operation. The same conclusion can be obtained from the other scenes. It is also consistent with the visual effect. Therefore, the noise can be filtered effectively on the premise of keeping the resolution undegraded with the methods proposed in the paper.

6 CONCLUSIONS

With the experiences of frequency domain filtering methods for periodic noise in optical image, the filtering methods for bright and shadow stripe noise in burst mode SAR image are studied and a one-dimensional weighted median filter in frequency domain independent of the parameters of SAR system is proposed in the paper. The validity of this method is proved by the processing of ENVISAT SAR data. For the irregular stripe noise caused by radar system itself, based on the theory foundation that the distributions of amplitude in spectrum image and grayscale image are perpendicular. An interactive two-dimensional frequency domain area filtering algorithm is proposed in the paper. The validity of this method is also proved by the processing of actual spaceborne SAR data.

REFERENCES

Aizenberg I and Butakoff C. 2008. A windowed Gaussian notch filter for quasi-periodic noise removal. *Image and Vision Computing*, **26**(10): 1347–1353

Chang C C, Hsiao J Y and Hsieh C P. 2008. An adaptive median filter for image denoising. IEEE Second International Symposium on Intelligent Information Technology Application, **2**: 346–350

Chen J S, Shao Y, Guo H D, Wang W M and Zhu B Q. 2003. Destriping CMODIS data by power filtering. *IEEE Trans. on GRS*, **41**(9): 2119–2124

Cumming I G and Wong F H. 2005. Digital Processing of Synthetic Aperture Radar Data: Algorithms and Implementation. Norwood: Artech House Inc

Curlander J C and McDonough R N. 1991. Synthetic Aperture Radar, Systems and Signal Processing. New York: Wiley & Sons, Inc

Ding D, Wang Z S, Jing L J, Xu Y J and Xie L B. 2002. Study of space-borne ScanSAR image processing. *Journal of Remote Sensing*, **6**(4): 259–265

Ghada A, Al Hudhud and Turner J. 2005. Digital removal of power frequency artifacts using a Fourier space median filter. *IEEE Signal Processing Letters*, **12**(8): 573–576

Gonzalez R and Woods R. 2001. Digital Image Processing (2nd edition), Englewood Cliffs, NJ: Prentice Hall

Hlzner J and Bamler R. 2002. Burst mode and ScanSAR interferometry. *IEEE Transaction on Geoscience and Remote Sensing*, **40**(9): 1917–1934

Lin T C. 2007. A new adaptive center weighted median filter for suppressing impulsive noise in images. *Information Sciences*, **177**(4): 1073–1087

Liu J G and Gareth L K M. 2006. FFT selective and adaptive filtering for removal of systematic noise in ETM+ Imageodesy Images. *IEEE Transaction on Geoscience and Remote Sensing*, **44**(12): 3716–3724

Lou X G, Li X L, Wang Z S. 1999. Stripe noise elimination of SAR pictures. *Journal of Image and Graphics*, **3**(4): 252–255

Preesan R, Wataru T and Yoshiffunmi Y. 2009. Restoration of Aqua MODIS band 6 using histogram matching and local least squares fitting. *IEEE Transaction on Geoscience and Remote Sensing*, **47**(2): 613–626

Tsai F and Chen W W. 2008. Striping noise detection and correction of remote sensing images. *IEEE Transaction on Geoscience and Remote Sensing*, **46**(2): 4122–4130

Zhang S Q and Mohammad A. K. 2002. A new impulse Detector for switching median filters. *IEEE Signal Processing Letters*, **9**(11): 360–363

SAR 图像中不同特性条纹噪声的滤除

寇光杰[1,2,3], 王贞松[1], 姚萍[1]

1. 中国科学院 计算技术研究所, 北京 100190;
2. 中国科学院研究生院, 北京 100049;
3. 鲁东大学 信息科学与工程学院, 山东 烟台 264025

摘 要: 分析 Burst 工作模式星载 SAR 系统中, 采用全孔径成像算法会产生周期性明暗条纹噪声的原因, 提出一种简单高效的一维频域滤除算法, 并给出包含该操作的改进距离多普勒成像算法流程。对于因雷达系统本身原因而产生的一些非周期不规则条纹噪声进行讨论, 针对此类噪声提出一种二维频域区域滤波的算法。通过对实际星载 SAR 数据的处理, 验证算法的有效性。

关键词: 距离多普勒算法, 条纹噪声, 频域滤波, Burst 工作模式

中图分类号: TP751/TN958 **文献标志码:** A

引用格式: 寇光杰, 王贞松, 姚萍. 2011. SAR 图像中不同特性条纹噪声的滤除. 遥感学报, 15(1): 1–12
Kou G J, Wang Z S and Yao P. 2011. Filtering methods for different characteristic stripe noise in SAR image. *Journal of Remote Sensing*, 15(1): 1–12

1 引 言

星载合成孔径雷达(SAR)是一种全天时、全天候工作的主动式微波传感器, 已经广泛应用到对地观测的各领域。由于所用信号处理算法或雷达系统本身的原因, 有时在所生成的 SAR 图像上会出现一些周期性或非周期性条纹噪声, 严重影响了图像质量及后期应用。因此寻找简单有效的 SAR 图像噪声滤除算法具有重要意义。而 SAR 的相干成像原理又使得其图像特性与光学图像不同, 比如存在乘性相干斑噪声。这就使得常用的光学图像降噪算法不能直接应用到 SAR 图像的处理中。对于 SAR 图像的条纹噪声, 娄晓光等 (1999)曾经进行过一些研究, 本文在此基础上进一步根据 SAR 图像中条纹噪声的不同特性进行分类, 提出两种更加简单高效的降噪算法。

首先借鉴光学图像处理中对周期性噪声滤除的方法(Aizenberg 等, 2008; Chen 等, 2003; Ghada 等, 2005; Preesan 等, 2009; Tsai 等, 2008; Liu 等, 2006), 提出一种简单高效的一维频域加权中值滤波算法。该算法通过频域多条方位线取均值来确定条纹噪声所对应的频率, 从而最大限度的降低 SAR 图像中相干噪声的干扰。此算法可以有效滤除 Burst 模式星载 SAR 数据采用全孔径算法处理时, 产生的沿方位向垂直分布的周期性明暗条纹噪声(Cumming 等, 2005; Hlzner 等, 2002)。在计算效率上此算法也比传统二维频域滤波算法有较大提高, 并且可以方便地将其融入到 RD(Range Doppler, RD)成像算法中。文中给出改进后 RD 算法的流程图, 并通过对 ENVISAT SAR 实际雷达数据的处理验证算法的有效性。

在分析时域灰度图像和频域幅度图像之间的对应关系后, 提出第二种交互式二维频域区域滤波算法。该算法可以有效处理因 SAR 系统本身或外界干扰等原因, 而产生的一些更加复杂的非周期不规则条纹干扰。最后通过对实际星载 SAR 图像的处理验证该算法的有效性。

2 条纹噪声滤除算法的理论基础

二维傅里叶变换是一种正交变换, 它可以将图像分解为一系列正弦和余弦信号, 因此在图像的分

收稿日期: 2010-01-21; **修订日期:** 2010-06-02

基金项目: 国家十一五预研项目。

第一作者简介: 寇光杰(1977—), 男, 讲师, 博士, 毕业于中国科学院计算技术研究所, 目前主要从事 SAR 信号处理及图像处理等方面的研究。E-mail: kouguangjie@ict.ac.cn。

析、滤波、压缩和重建等方面得到广泛应用。该变换使能量分布向低频成分方向集中，而图像上的边缘、线条等细节信息在高频成分上得到体现。若图像中目标形状或排列呈现某种方向性，那么具有较高值的幅度谱也会呈现出与目标方向正交的方向性(娄晓光等, 1999; Gonzalez 等, 2001)。该结论可从理论上加以证明。若时域图像 $f(x,y)$的灰度分布模式沿 y 轴延伸，不妨用式(1)来表示。

$$f(x,y)=\begin{cases}\boldsymbol{A} & 0\leqslant x\leqslant \boldsymbol{X},0\leqslant y\leqslant \boldsymbol{Y}\\ 0 & \text{其他}\end{cases} \tag{1}$$

式中，$\boldsymbol{A}$ 为图像灰度值，$\boldsymbol{X}$、$\boldsymbol{Y}$ 分别为图像沿横纵坐标的像元数，且 $\boldsymbol{X}<<\boldsymbol{Y}$。则 $f(x,y)$的傅里叶变换结果为

$$F(u,v)=AXY\times\left|\frac{\sin(\pi u\boldsymbol{X})\times\exp(-j\pi u\boldsymbol{X})}{\pi u\boldsymbol{X}}\right|\times\left|\frac{\sin(\pi v\boldsymbol{Y})\times\exp(-j\pi v\boldsymbol{Y})}{\pi v\boldsymbol{Y}}\right| \tag{2}$$

其幅度谱可表示为

$$|\boldsymbol{F}(u,v)|=\boldsymbol{AXY}\times\left|\frac{\sin(\pi u\boldsymbol{X})}{\pi u\boldsymbol{X}}\right|\times\left|\frac{\sin(\pi v\boldsymbol{Y})}{\pi v\boldsymbol{Y}}\right| \tag{3}$$

因为 $1/\boldsymbol{X}>>1/\boldsymbol{Y}$，所以幅度谱函数模式沿 u 轴延伸。这也就是说图像幅度谱模式延伸方向与原图像灰度分布延伸方向相互正交。由二维傅里叶变换的尺度变换性质式(4)和旋转特性式(5)可以证明，对于图像中的一般模式上述结论也同样成立。

$$\mathrm{FFT}\{f(\boldsymbol{a}x,\boldsymbol{b}y)\}=\frac{\boldsymbol{F}(u/\boldsymbol{a},v/\boldsymbol{b})}{|\boldsymbol{ab}|} \tag{4}$$

$$\mathrm{FFT}\{f(x\cos\boldsymbol{\theta}-y\sin\boldsymbol{\theta},x\sin\boldsymbol{\theta}+y\cos\boldsymbol{\theta})\}=\boldsymbol{F}(u\cos\boldsymbol{\theta}-v\sin\boldsymbol{\theta},u\sin\boldsymbol{\theta}+v\cos\boldsymbol{\theta}) \tag{5}$$

式中，$FT\{f\}$为函数 $f(x,y)$的二维傅里叶变换，a、b、θ 为常量。这样可由时域图像中噪声形状推测出其频域幅度模式的形状，然后再进行相应处理即可达到降噪目的。这也是本文构造频域噪声滤波器的出发点。

3 SAR 图像周期性条纹滤除

3.1 周期性条纹噪声分析

采用全孔径方法处理 Burst 模式星载 SAR 数据时，首先要对 Burst 数据之间进行适当补零，以使各个Burst之间满足条带模式原始数据的时序关系，然后即可采用条带式成像算法进行处理。这种补零等效于连续条带模式的数据与固定持续时间矩形信号(值为零)相乘，从而额外增加一个沿方位向分布的固定周期噪声信号，该噪声信号对于距离向方位向解耦后，再进行匹配滤波的成像算法(如RD)影响很大，最终在所生成的SAR图像上产生一系列明暗相间的条纹(Curlander 等, 1991; Ding 等, 2002; Hlzner 等, 2002)。这与天线方向图不均匀加权所产生的影响有一定相似性。因该条纹噪声沿距离向延伸，且在方位向上周期性出现。由第 2 节结论可知，此条纹噪声对应频谱模式将沿方位向延伸。

如果该明暗条纹的周期及条纹宽度是确定的，则此噪声对应二维频域幅度图像中两个沿方位向对称的脉冲，其中脉冲所对应的频率由条纹噪声的周期决定。采用传统光学图像处理方法，可以在二维频域采用陷波滤波器(Gonzalez 等, 2001)，加窗高斯陷波滤波器(Aizenberg 等, 2008)或中值滤波器(Ghada 等, 2005; Zhang 等, 2002; Lin 等, 2007; Chang 等, 2008)将该噪声滤除掉。由于此明暗条纹具有周期性和规则的形状，则降噪处理时无需将图像完全变换到二维频域，只需沿垂直条纹噪声的方向进行一维傅里叶变换即可，为此提出 SAR 图像周期性条纹噪声一维频域滤除算法。

3.2 周期性条纹噪声滤除

因为SAR图像中的条纹噪声和自然场景产生的频谱能量混合在一起，并且还有乘性噪声的影响，所以单独一条方位向频谱线不能准确定位噪声所对应频率。若将各行频谱幅度序列对应累加，则自然场景对应的频谱能量将会相互抑制，使得最终累加和不会太大，而周期性条纹噪声对应频率处的能量累加和将会出现峰值。这样除了零频处最高峰值之外的其余峰值即可能是条纹噪声所对应的频率。则一维频域条纹噪声滤除算法步骤如下：

假定待处理图像方位向为 $\boldsymbol{M}$ 点，距离向为 $\boldsymbol{N}$ 点；向量 $\boldsymbol{F}_x$ 表示第 x 条方位线的傅里叶变换结果，$\boldsymbol{P}_x$ 表示相应频谱幅度值，其中 x=1,…,N:

(1) 由式(6)求出方位线频谱幅度的均值。

$$\boldsymbol{MeanSpect}=\frac{1}{N}\times\sum_{x=1}^{N}\boldsymbol{P}_x \tag{6}$$

其中

$$\boldsymbol{P}_x=|\boldsymbol{F}_x| \tag{7}$$

$$\boldsymbol{F}_x(v)=\frac{1}{M}\times\sum_{y=0}^{M-1}f(x,y)\times\exp(-j2\pi vy/M) \tag{8}$$

(2) 对 ***MeanSpect*** 求取零频以外的峰值。

利用一维向量 ***MeanSpect***，找到二个关于零频对称的最高幅度峰值，它们对应的频率就是此处条纹噪声对应的频率，不妨用 f_{noise} 统一表示。这种搜索峰值来确定噪声频率的方法，不依赖于 SAR 系统的任何参数，且不受图像重采样的影响，使得去条

纹噪声成为一种通用的处理操作。

(3) 根据得到的噪声频率 f_{noise} 利用式(9)所示一维中值波滤波器对每条方位线进行处理。

$$\boldsymbol{F}(f_{\text{noise}}) = \text{median}\{\boldsymbol{F}(v)/\delta\} \tag{9}$$

式中, median 为取中值函数, 将每条方位线在 f_{noise} 处的幅度值取作左右两侧一定窗口范围内的中间值, 而相位保持不变。δ为一加权因子。因为在噪声对应频率上也会有一部分实际图像的信息, 所以如果直接将此频率对应的能量置为零, 则会有一部分图像信息丢失。为了在去除条纹噪声的同时尽量保持图像的原有信息, 此处噪声滤除选择了加权一维中值滤波的方法。

(4) 将处理后的方位向频域图像进行逆傅里叶变换, 即可得到滤除噪声后的图像。

3.3 含条纹滤除操作的改进 RD 算法

上述滤除条纹噪声的操作在一维频域即可实现, 通过分析 RD 算法的流程不难发现, 若将噪声的滤除操作放在 RD 成像算法最后一步方位向逆傅里叶变换之前, 则可以完成同样的功能, 使得总体计算效率又得到较大的改善。图 1 给出改进前后的 RD 成像算法流程。

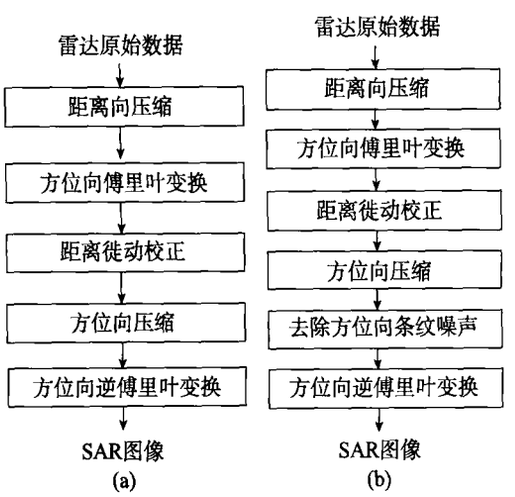

图 1 改进前后 RD 算法流程

(a) 传统 RD 算法; (b) 改进 RD 算法

另外, 如果通过成像过程来滤除方位向周期性条纹噪声, 则 SAR 系统的主要雷达参数: Burst 持续时间、PRF、补零对应时间等都是可以获得的。这时条纹噪声对应的频率可通过简单计算直接求出, 不再通过各方位线频谱累加的处理方法进行计算。

4 不规则条纹噪声滤除

4.1 不规则条纹噪声的分析

由于雷达系统本身的原因或者外界干扰等因素, 有时会在 SAR 图像中产生另外一种类型的条纹噪声。这种噪声的典型特点是没有周期性, 与地面目标相关, 并且条纹的长短及宽度都是变化的。因为条纹噪声长短不一并且不是贯穿整幅图像, 所以采用第 3 节方法确定不了噪声频率, 并且此时传统二维频域的滤波方法(Gonzalez 等, 2001; Aizenberg 等, 2008; Ghada 等, 2005)也不再有效。为此本文提出二维频域区域滤波算法: 首先由第 2 节图像频域幅度分布与时域灰度分布正交的结论, 在频谱图像中确定出噪声对应区域, 然后再对该区域进行相应处理, 从而达到去除条纹噪声的目的。

4.2 频域幅度图像中噪声对应区域的确定

虽然此类条纹噪声看上去非常杂乱, 但它们仍然具有一些共同特点: 沿着竖直方向延伸、没有周期性、各条纹宽度是变化的。由第 2 节结论可知, 此类条纹噪声在二维频谱图像中的能量模式应该沿水平方向延伸, 又因为各条纹没有固定周期, 故在水平方向各频率上均可能有较高能量出现, 所以此类噪声应该在频域图像中产生水平方向亮线。另外, 每一条噪声条纹的宽度又是不同的, 所以它们对应频域图像中的水平方向亮线应该有一定宽度。基于这种原理可以非常容易的确定出噪声在频域幅度图像中的对应区域。这样噪声的滤除工作就转化为在频域中对该区域的数据进行适当调整的操作。

4.3 不规则条纹噪声滤除算法的具体步骤

(1) 对所要处理图像进行二维快速傅里叶变换, 并绘出相应频谱幅度图(为看清细节可先对幅度图进行对数变换, 然后再显示)。

(2) 由(1)所得频谱幅度图确定出竖直条纹噪声对应频谱幅度图中的区域。

(3) 保持相位不变, 将噪声所对应区域的幅度谱数值用该区域两侧一定范围内的幅度谱均值来替代。

(4) 将处理后频域图像进行快速逆傅里叶变换, 即可得到滤除噪声后的图像。

5 实 验

5.1 SAR 图像周期性条纹噪声滤除

ENVISAT 卫星是欧空局的对地观测卫星系列之一, 于 2002-03-01 发射升空。在 ENVISAT-1 卫星上载有多个传感器, 分别对陆地、海洋、大气进行观测, 其中最主要的就是合成孔径雷达传感器 ASAR。ASAR 工作在 C 波段, 具有多极化、可变观

测角度、宽幅成像等特性。图 2 为对其 Burst 模式原始数据采用全孔径 RD 算法所生成的 level 1A 级图像及去噪结果。

图 2(a)(d)给出了含有条纹噪声的 SAR 图像，可以看出沿方位向存在明显的周期性能量起伏，造成图像质量严重下降。图 2(b)(e)为采用第 3 节算法滤除噪声后的结果，此处一维中值滤波采用的窗口大小为 7, δ=5。图 2(c)(f)示意了滤除掉的周期性噪声。图 3 给出了场景 1 滤除噪声前后方位向频谱均值向量 ***MeanSpect*** 的变化，其中横坐标为归一化频率，图中只画出了半个周期的频谱曲线。图 3(b)中噪声对应峰值已被有效去除。

5.2 SAR 图像不规则条纹噪声的滤除

图 4 为星载 SAR 条带模式下得到的迪拜某地区雷达数据，采用 RD 算法成像后的 level 1A 级图像。其中图 4(a)(d)为含有条纹噪声的图像，虽然条纹噪声看上去间隔较小，但是如果直接采用低通滤波器将不会获得好的效果，图 4(i)显示了图 4(a)经过高斯低通滤波处理后的图像，虽然图像已经变的非常模糊，但是条纹噪声仍然未得到有效滤除。所以对于这类噪声低通滤波器是无效的。当然若此时再采用

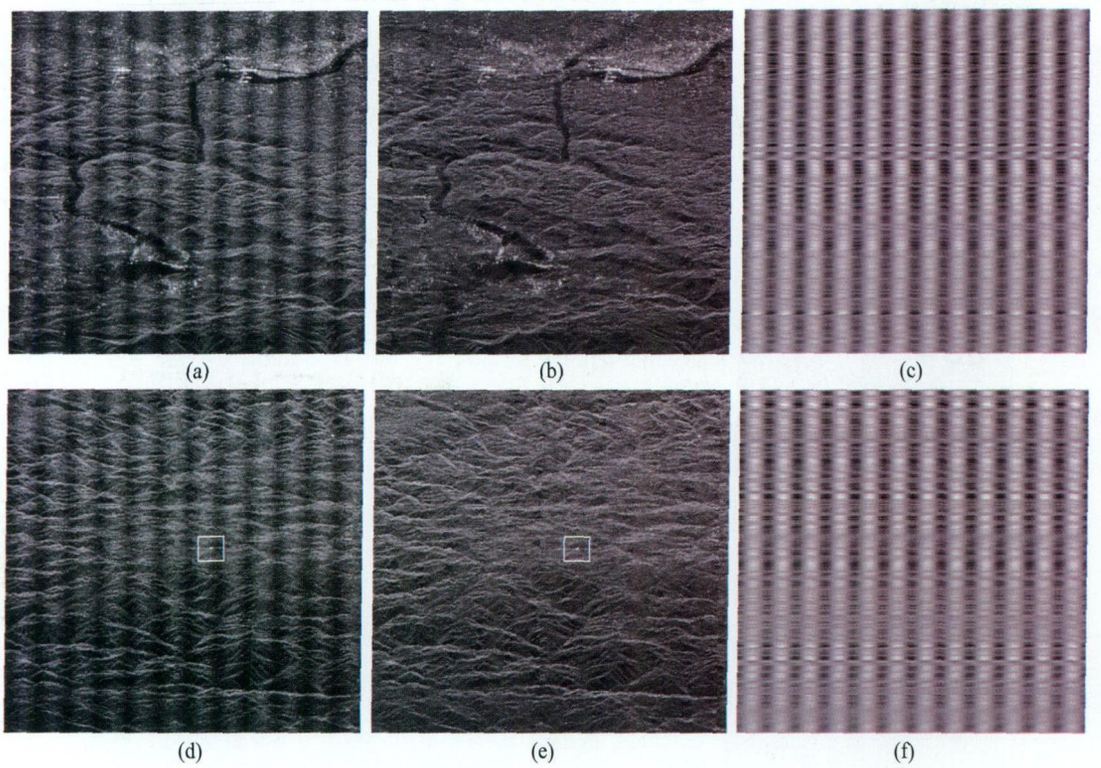

图 2 周期性条纹噪声滤除结果(图像为 512×512)

(a) 场景 1 滤除条纹噪声前; (b) 场景 1 滤除噪声后; (c) 场景 1 滤除掉的噪声; (d) 场景 2 滤除条纹噪声前; (e) 场景 2 滤除噪声后; (f) 场景 2 滤除掉的噪声

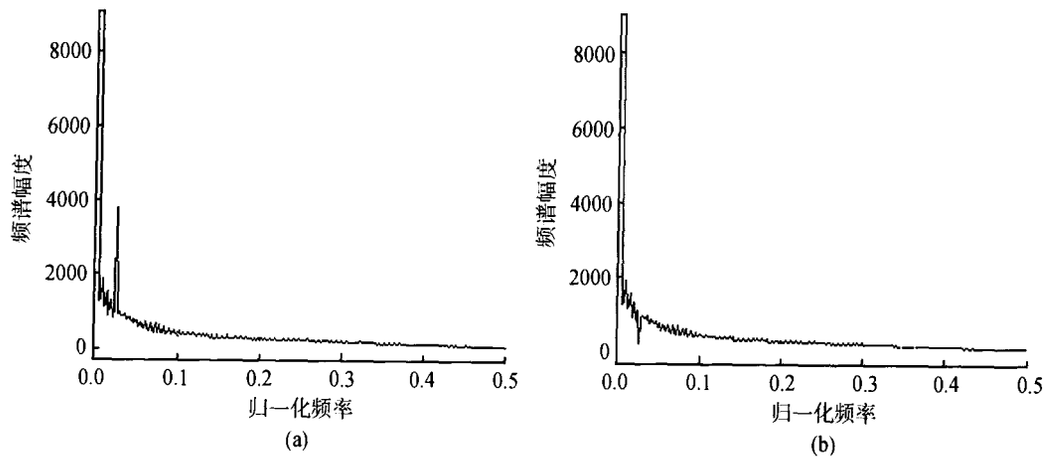

图 3 场景 1 噪声滤除前后方位向频谱均值的变化

(a) 含条纹噪声的方位向频谱; (b) 滤除条纹噪声后方位向频谱

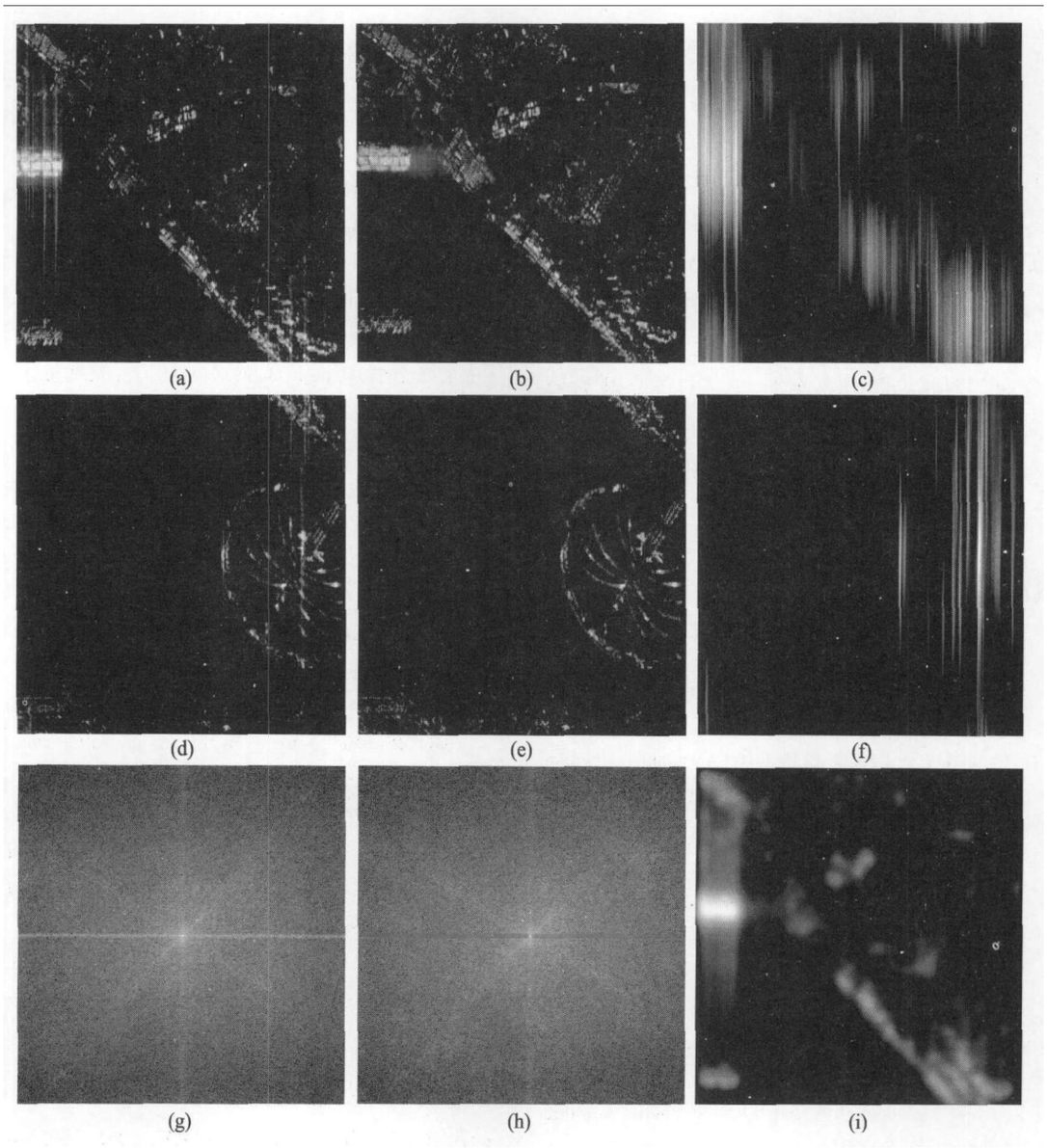

图 4 非周期性条纹噪声滤除结果(图像为 256×256)

(a) 场景 3 滤除条纹噪声前; (b) 场景 3 滤除噪声后; (c) 场景 3 滤除掉的噪声;(d) 场景 4 滤除条纹噪声前; (e) 场景 4 滤除噪声后; (f) 场景 4 滤除掉的噪声; (g) 场景 3 降噪前频谱幅度图; (h) 场景 3 降噪后频谱幅度图; (i) 场景 3 低通滤波处理后结果

3.2 节一维频域滤波的方法将会发现累加后各频率处的幅度不存在明显峰值, 从而无法确定噪声对应的频率, 这也进一步验证了 4.1 节的分析。图 4(b)(e)为采用 4.3 节算法去除条纹噪声后的结果, 图 4(c)(f)为滤除掉的噪声。显然此时条纹噪声已经得到了有效滤除。图 4(g)(h)为图 4(a)滤除条纹噪声前后的二维频谱幅度图像。

5.3 降噪效果评价

除图像的视觉效果外, 本文还用了噪声去除率(noise reduction ratio, *NR*) (Preesan 等, 2009; Chen 等, 2003)和分辨率变化量来对降噪算法进行评价。*NR* 可由式(10)来计算。

$$NR = N_0 / N_k \tag{10}$$

式中, N_0 表示原始图像中条纹噪声对应频率处的能量, N_k 为降噪后相应频率处的能量。*NR* 反映了噪声去除程度的强弱。上述 4 幅图像的 *NR* 值如表 1 所示。

表 1 噪声去除率 *NR*

图像	*NR*	图像	*NR*
场景 1	18.69	场景 3	26.36
场景 2	19.17	场景 4	19.26

分辨率变化量是通过测量图像中强散射目标在降噪前后所占像元数是否有变化来实现的。如场景 2 中方形区域所示的 20×20 区域中强散射目标在降噪前后均为 8 个像素, 即去条纹噪声的操作并未使分辨率明显下降。对其余场景采用同样方法测量后, 也可得到相同的结论。这也与视觉效果相一致, 所以本文降噪算法可以实现在保持图像分辨率的前提下有效去除条纹噪声。

6 结 论

借鉴光学图像中对周期性噪声的频域滤除方法，对 Burst 模式星载 SAR 图像中明暗条纹噪声的滤除进行了研究，提出一种不依赖于 SAR 系统参数的一维频域加权中值滤波方法，通过对 ENVISAT 实际雷达数据的处理验证了算法的有效性。针对雷达系统本身原因而引入的不规则条纹噪声，以频域幅度图像延伸方向与时域灰度图像延伸方向的正交性为理论依据，提出一种二维频域区域滤波的交互式降噪算法，通过对实际星载 SAR 图像的处理验证该算法的有效性。

REFERENCES

Aizenberg I and Butakoff C. 2008. A windowed Gaussian notch filter for quasi-periodic noise removal. *Image and Vision Computing*, **26**(10): 1347–1353

Chang C C, Hsiao J Y and Hsieh C P. 2008. An adaptive median filter for image denoising. IEEE Second International Symposium on Intelligent Information Technology Application, **2**: 346–350

Chen J S, Shao Y, Guo H D, Wang W M and Zhu B Q. 2003. Destriping CMODIS data by power filtering. *IEEE Trans. on GRS*, **41**(9): 2119–2124

Cumming I G and Wong F H. 2005. Digital Processing of Synthetic Aperture Radar Data: Algorithms and Implementation. Norwood: Artech House Inc

Curlander J C and McDonough R N. 1991. Synthetic Aperture Radar, Systems and Signal Processing. New York: Wiley & Sons, Inc

Ding D, Wang Z S, Jing L J, Xu Y J and Xie L B. 2002. Study of space-borne ScanSAR image processing. *Journal of Remote Sensing*, **6**(4): 259–265

Ghada A, Al Hudhud and Turner J. 2005. Digital removal of power frequency artifacts using a Fourier space median filter. *IEEE Signal Processing Letters*, **12**(8): 573–576

Gonzalez R and Woods R. 2001. Digital Image Processing (2nd edition), Englewood Cliffs, NJ: Prentice Hall

Hlzner J and Bamler R. 2002. Burst mode and ScanSAR interferometry. *IEEE Transaction on Geoscience and Remote Sensing*, **40**(9): 1917–1934

Lin T C. 2007. A new adaptive center weighted median filter for suppressing impulsive noise in images. *Information Sciences*, **177**(4): 1073–1087

Liu J G and Gareth L K M. 2006. FFT selective and adaptive filtering for removal of systematic noise in ETM+ Imageodesy Images. *IEEE Transaction on Geoscience and Remote Sensing*, **44**(12): 3716–3724

Lou X G, Li X L, Wang Z S. 1999. Stripe noise elimination of SAR pictures. *Journal of Image and Graphics*, **3**(4): 252–255

Preesan R, Wataru T and Yoshiffunmi Y. 2009. Restoration of Aqua MODIS band 6 using histogram matching and local least squares fitting. *IEEE Transaction on Geoscience and Remote Sensing*, **47**(2): 613–626

Tsai F and Chen W W. 2008. Striping noise detection and correction of remote sensing images. *IEEE Transaction on Geoscience and Remote Sensing*, **46**(2): 4122–4130

Zhang S Q and Mohammad A. K. 2002. A new impulse Detector for switching median filters. *IEEE Signal Processing Letters*, **9**(11): 360–363

附中文参考文献

丁丁，王贞松，荆麟角，徐永健，谢列宾. 2002. 星载 ScanSAR 成像研究. 遥感学报, **6**(4): 259–265

娄晓光，李象霖，王贞松. 1999. SAR 图像中条纹干扰的抑制. 中国图象图形学报, **3**(4): 252–255